

# The red clump absolute magnitude based on revised Hipparcos parallaxes

M. A. T. Groenewegen

Koninklijke Sterrenwacht van België, Ringlaan 3, 1180 Brussels, Belgium  
e-mail: marting@oma.be

Received 15 May 2008 / Accepted 26 June 2008

## ABSTRACT

*Context.* Over the past decade the use of the red clump (RC) as distance indicator has increased in importance as this evolutionary phase is well populated and a good local calibration exists.

*Aims.* The absolute calibration of the RC in the *I* and *K* band is investigated again based on the recently published revised Hipparcos parallaxes.

*Methods.* A numerical model is developed that takes the various selection criteria and the properties of the Hipparcos catalogue into account. The biases involved in applying certain selections are estimated with this model.

*Results.* The absolute magnitudes that are found are  $M_I = -0.22 \pm 0.03$  and  $M_K = -1.54 \pm 0.04$  (on the 2MASS system). The *I*-band value is in good agreement with previous determinations, the *K*-band value is fainter than previously quoted, and this seems to be related to a selection bias whereby accurate *K*-magnitudes are only available for relatively few bright stars. Applying population corrections to the absolute *K* magnitude of RC stars in clusters supports the fainter magnitude scale.

**Key words.** stars: distances – cosmology: distance scale

## 1. Introduction

Paczyński & Stanek (1998) were the first to advocate the use of red clump (RC) stars in the *I*-band as distance indicators. Two advantages are that this phase of stellar evolution is usually well populated, and that many RC stars exist with good parallaxes in the Hipparcos catalogue.

They consider stars with an error in parallax smaller than 10%, located in the box  $0.8 < (V - I) < 1.25$  and  $-1.4 < M_I < 1.2$  and with Hipparcos flag H42 equal to one of “A, C, E, F, G”, which means that the star has one or more *I*-band measurements in the Cousins, Johnson, or Kron-Eggen system. They find no significant trend of  $M_I$  on colour and derived  $M_I = -0.185 \pm 0.016$  for the entire sample. They then considered the 228 stars with  $d < 70$  pc and average distance of 50 pc to find  $M_I = -0.192 \pm 0.023$ , and  $M_I = -0.094 \pm 0.027$  for the rest of the sample at an average distance of 106 pc. The difference is ascribed to reddening, and when extrapolating to 0 pc, they arrive at their final result of find  $M_I = -0.279$  and assign an error bar of 0.088. In deriving these number, they also applied a correction for “a distance bias”.

Stanek & Garnavich (1998) considered the same sample, and their final value of  $M_I = -0.23 \pm 0.03$  is based on the sub sample of stars within 70 pc and they argue that no correction for reddening is needed, and they do not apply a correction for selecting the sample on parallax.

Udalski (2000) considered the effect of metallicity. He took the same cut in parallax error and Hipparcos H42 flags, but also included stars with flag “H” to increase the sample and considered stars with a metallicity determination from high-resolution spectroscopy by McWilliam (1990). Based on this sample of 284 stars, he finds a weak dependence on metallicity:  $M_I = (0.13 \pm 0.07)([Fe/H]+0.25) + (-0.26 \pm 0.02)$ .

Alves (2000) was the first to consider the *K*-band for RC stars as a standard candle. He considered the 284 stars from Udalski (2000) and finds that 238 of them have a *K*-magnitude in the Two Micron Sky Survey (TMSS, Neugebauer & Leighton 1968; stars are designated by “IRC” numbers). Assuming no reddening and considering stars with  $-2.5 < M_K < -0.8$  and all  $(V - K)$  colours, he finds  $M_K = -1.61 \pm 0.03$  and a weak dependence on metallicity  $M_K = (0.57 \pm 0.36)[Fe/H] + (-1.64 \pm 0.07)$ .

The RC has gained importance as a distance indicator since the Paczyński & Stanek (1998) paper as shown for example by distance estimates based on the RC to Fornax (Rizzi et al. 2007), M 33 (Kim et al. 2002), or IC 1613 (Dolphin et al. 2001).

With the recent publication of the revised Hipparcos parallax data, it is timely to investigate the absolute magnitude of the RC again. In Sect. 2 the revised Hipparcos data is introduced with auxiliary data used in the analysis. Section 3 describes the numerical model used for estimating selection biases. Section 4 describes the results, and Sect. 5 presents a brief summary and discussion.

## 2. The data

The Hipparcos data used are the parallax and error in the parallax from the re-reduction of the raw data by van Leeuwen (2007). For other data (*V*, *I*, Hipparcos flags), the originally published catalogue is used (ESA 1997).

Using the script submission tool within VizieR (Ochsenbein et al. 2000) the list of Hipparcos objects was correlated with selected measurements available, in particular, spectroscopic  $[Fe/H]$  values (available for 2445 stars, and adding 11 stars from Zhao et al. 2001; 64 from Liu et al. 2001; and 178 from Mishenina et al. 2006), the TMSS catalogue (Neugebauer & Leighton 1969, available for 3167 stars), and Strömgren

photometry (available for 36 337 stars). In case of multiple [Fe/H] determinations the mean was taken.

Independently, the Hipparcos objects are correlated on position with the DENIS (Epchtein et al. 1999, for 42 696 stars) and 2MASS (Skrutskie et al. 2006, for 117 358 stars) NIR catalogues. The TMSS was the main source of  $K$ -magnitudes used by Alves (2000). This is the only source of uniform  $K$ -magnitude for bright objects that often saturate in the DENIS and 2MASS surveys. In the present study TMSS, DENIS and 2MASS are being used but this requires transformation to the 2MASS system, which will be the system of choice. Using 749 objects with a 2MASS photometric quality flag, phqual-flag, of ‘‘A’’ in the  $K$ -band and that not saturate in DENIS  $I$  (implying  $I > 10$ ) it is found that DENIS  $K - 2MASS K = -0.018 \pm 0.066$  with no colour term on  $(I - K)_{\text{DENIS}}$ . There are no stars in common between the TMSS survey and non-saturated DENIS or 2MASS objects with phqual-flags of ‘‘A’’ or ‘‘B’’ in  $K$ . The transformation to the 2MASS system is done indirectly via the SAO Carter (1990) system. The advantage over a comparison to the Koornneef (1983) system, which was used by Alves (2000), is that the colour term and offset with respect to the 2MASS system are smaller (Carpenter 2001, and updated on the IPAC website<sup>1</sup>).

Using 62 TMSS stars that are listed in Carter (1990) and that have both an IRC  $K$  and  $I$  magnitude available, the following relations are derived:  $(J - K)_{\text{Carter}} = 0.484(I - K)_{\text{IRC}} - 0.103$  with a dispersion of 0.04 mag, and eliminating 5 outliers,  $K_{\text{Carter}} - K_{\text{IRC}} = -0.011$  with no significant colour term, and with a dispersion of 0.04 mag. The transformation from the Carter to the 2MASS system follows the relation on the quoted IPAC website:  $K_{2\text{mass}} = K_{\text{Carter}} - 0.024 + 0.017(J - K)_{\text{Carter}}$ .

The adopted  $K$ -band magnitude is, in order of preference, (1) the 2MASS value, but only when phqual is ‘‘A’’; (2) The DENIS value (for non-saturated stars with  $I_{\text{denis}} > 10$ ) corrected by +0.018 mag; (3) the TMSS/IRC value, transformed to the 2MASS system as described above. If no  $I_{\text{IRC}}$  is available a mean colour for RC stars of  $(I - K)_{\text{IRC}} = 1.55$  is used in the transformation.

Of all Hipparcos stars that have a  $K$ -magnitude assigned, 3116 are based on TMSS, 17 on Denis and 103827 on 2MASS.

### 3. The model

In this section a model is described to construct synthetic samples of stars and apply various selection criteria in order to generate samples of stars that closely resemble in nature the observed data. The model follows largely Groenewegen & Oudmaijer (2000) but is based on the properties of the revised Hipparcos catalogue.

#### 3.1. Galactic model

The coordinate system used is cylindrical coordinates centred on the Galactic centre. The galactic distribution is assumed to be a double exponential disk with a scale height  $H$  in the  $z$ -direction (the coordinate perpendicular to the galactic plane), and a scale length  $R_{\text{GC}}$  in the galacto-centric direction. The distance to the Galactic centre is taken to be 7800 pc (Zucker et al. 2006).

**Table 1.** Comparison of different reddening models.

	Drimmel et al.	Parenago	Arenou et al.
Marshall et al.	$1.01 \pm 0.82$	$1.00 \pm 0.88$	$0.99 \pm 0.76$
Arenou et al.	$1.20 \pm 0.62$	$1.15 \pm 0.55$	–
Parenago	$1.06 \pm 0.24$	–	–

#### 3.2. Luminosity function

The luminosity function can be arbitrary but, in the case of simulating RC stars, is assumed to be a Gaussian. In  $I$  with a mean  $M_I = -0.27$  and  $\sigma$  of 0.20. The  $(V - I)$  colours is assumed to be a Gaussian with mean 0.98 and  $\sigma = 0.085$ . In  $K$  the Gaussian has a mean  $M_K = -1.60$  and  $\sigma$  of 0.22, while the  $(V - K)$  colours is taken as a Gaussian with mean 2.32 and  $\sigma$  of 0.21.

#### 3.3. Reddening

Visual extinction in the simulation and to de-redden the observations is based on several 3-dimensional reddening models available in the literature. Marshall et al. (2006) presents reddening in the  $K$ -band with  $15'$  sampling along 64 000 lines-of-sight in the direction  $|l| \leq 100$  deg and  $|b| \leq 10$  deg based on 2MASS data. Drimmel et al. (2003) presents a reddening model based on the dust distribution model of Drimmel & Spergel (2001), which is based on COBE/DIRBE data. Arenou et al. (1992) presents a reddening model based on a comparison of observed  $B, V$  photometry with predicted photometry from a star’s spectral type. Finally, a simple law following Parenago (1940) was considered:

$$A_V = 0.097/|\sin b| (1.0 - \exp(-0.0111 d |\sin b|)). \quad (1)$$

The Marshall et al. results have been taken as reference model, and their reddenings were transformed to  $A_V$  as  $A_K/0.12$ .

However, this model is only available over a limited range in galactic coordinates, therefore a Monte Carlo simulation was made to randomly generate galactic coordinates and distances assuming a constant number density of stars within 3 kpc distance of the Sun. If the galactic coordinates were within the range of applicability of the Marshall et al. model, the visual extinction from the other models was determined. In the end, using several 1000 positions, the average and dispersion in the various ratios between extinction models were calculated, and the results are in Table 1, in the sense model listed in the row divided by model listed in the column.

Although the dispersion in all the ratios is quite large, they mostly agree in the mean. It only seems that the Arenou et al. model gives higher extinction than the Drimmel et al. and Parenago model. The finally adopted visual extinction was the average of the models by Parenago, Drimmel et al., and Arenou et al. multiplied by 0.84.

#### 3.4. Properties of Hipparcos data

The adopted completeness function in  $H_p$  magnitude is

$$(1.0 + \exp((H_p - 8.695)/0.5206))^{-1.194}. \quad (2)$$

This was derived by comparing the observed magnitude distribution to that predicted with the TRILEGAL Galactic model (Girardi et al. 2005).

The completeness functions quoted below are derived by inspecting the ratio of stars that fulfil a particular selection to all

<sup>1</sup> [www.ipac.caltech.edu/2mass/releases/allsky/doc/sec6\\_4b.html](http://www.ipac.caltech.edu/2mass/releases/allsky/doc/sec6_4b.html)

stars, as a function of  $H_p$  magnitude. The completeness function of stars with  $I$ -band flags “A+C+E+F+G” is approximated as

$$\begin{array}{ll} 0.90 & H_p \leq 5 \\ 0.50 - 0.45(H_p - 5)/2 & 5 < H_p < 7 \\ 0.05 & H_p \geq 7. \end{array} \quad (3)$$

If stars with  $I$ -band flag “H” are also included, this becomes

$$\begin{array}{ll} 0.92 & H_p \leq 5 \\ 0.60 - 0.40(H_p - 5)/4 & 5 < H_p < 9 \\ 0.20 & H_p \geq 9. \end{array} \quad (4)$$

As outlined above,  $K$ -band magnitudes were to Hipparcos stars based on high-quality 2MASS and IRC data. The completeness function is approximated as

$$\begin{array}{ll} 0.60 & H_p \leq 5 \\ 0.69 & 5 < H_p \leq 7 \\ 0.69 + 0.30(H_p - 7)/1.5 & 7 < H_p < 8.5 \\ 0.99 & H_p \geq 8.5. \end{array} \quad (5)$$

For fainter objects, a (reliable)  $K$ -magnitude is available for almost all objects because of the all-sky nature of the 2MASS survey, but for brighter stars this is clearly not the case.

As outlined above, spectroscopic [Fe/H] values have been retrieved using VizieR and recent literature. The completeness function is approximated as

$$\begin{array}{ll} 0.55 & H_p \leq 4 \\ 0.55 - 0.53(H_p - 4)/3 & 4 < H_p < 7 \\ 0.02 & H_p \geq 7 \\ 0.0 & H_p \geq 8. \end{array} \quad (6)$$

The error on the  $H_p$  magnitude is small but has nevertheless been taken into account. The error is Gaussian distributed with the sigma value

$$\log \sigma_{H_p} = 0.290H_p - 5.510 \quad H_p > 11$$

$$\log \sigma_{H_p} = 0.177H_p - 4.265 \quad H_p \leq 11. \quad (7)$$

As explained in the explanatory supplement to the Hipparcos catalogue, stars with an ecliptic latitude more than 47 degree were observed more often, and this resulted in lower parallax errors on average. When  $\beta > 47^\circ$  the error on the parallax (in mas) is in the mean

$$\log \sigma_\pi = 0.1610H_p - 1.540,$$

with dispersion 0.075, and else

$$\log \sigma_\pi = 0.1573H_p - 1.368, \quad (8)$$

with dispersion 0.063. The minimum error on the parallax is

$$(\log \sigma_\pi)_{\min} = 0.1610H_p - 1.7. \quad (9)$$

In the simulation a parallax error is generated using the mean relation and the Gaussian dispersion. If this parallax error is above the minimum allowed value the star is retained.

The “measured” parallax is based on the true parallax (from the true distance) and the Gaussian distributed parallax error.

### 3.5. The model in practice

To begin with, a number of input parameters need to be set:

- scale length and scale height of the population;
- mean magnitude and dispersion in the luminosity function in the reference magnitude,  $\lambda$  (i.e.  $I$  or  $K$  in the present paper);
- mean magnitude and dispersion in the luminosity function in the  $(V - \lambda)$ -colour;
- $A_\lambda/A_V$  value and;
- the number of simulations, and number of stars per simulation.

The consecutive steps in the model are the following:

- Three random numbers are drawn to select the distance to the Galactic plane, the distance to the Galactic centre and a random angle  $\phi$  between 0 and  $2\pi$  in the Galactic plane centred on the Galactic centre. From this the distance  $d$  to the Sun is calculated. The galactic coordinates and ecliptic latitude is determined.
- From the properties of the observed sample (e.g. from the observed parallax, or a photometrically determined parallax), it is already possible to eliminate stars beyond a certain limiting distance.
- The reddening in the  $V$ -band and in the reference magnitude is determined.
- The true absolute magnitude in  $V$  and in the reference magnitude is determined.
- The true  $H_p$  magnitude is determined, from the distance,  $M_v$ ,  $A_v$ , and the fact that  $(H_p - V)$  is typically +0.1 (vol. 1, Sect 1.3, p. 59 of Hipparcos explanatory catalogue).
- The error in the  $H_p$  magnitude is determined and the observed  $H_p$  determined.
- The completeness function in  $H_p$  is determined, and a random number is generated to evaluate if the star is “observed”.
- Depending on the selection of the sample, other completeness functions are evaluated and applied.
- If the star is still “in”, Eqs. (8–9) are evaluated to determine the parallax errors, and the observed parallax.
- Depending on the selection of the sample, additional selection criteria on parallax or (relative) parallax error are applied.
- The observed magnitude in the reference colour is determined.
- The output of the model typically is the “observed” parallax, error in the parallax, true distance, photometric parallax based on the adopted absolute mean magnitude,  $H_p$ , observed reference magnitude,  $A_V$  and galactic coordinates.

## 4. The red clump

Table 2 lists the observed absolute magnitudes depending on various selections. These selections largely follow the selections made by previous works as quoted in the Introduction. In all cases, only stars where Hipparcos flag H30 (the goodness-of-fit) is  $< 5$ ,  $\pi > 0$ , and single stars (isoln = 5 as listed in the revised Hipparcos catalogue) are considered.

Following earlier work, stars are selected inside the box (all colours and magnitudes are understood to be de-reddened according to the model described in Sect. 3.3)  $0.75 < (V - I) < 1.25$ ,  $-1.6 < M_I < 1.2$ . The data is binned in absolute

**Table 2.** Results based on different sample selections.

Model	$\sigma_\pi/\pi$	<i>I</i> -flags	[Fe/H]	N	$M_I$	$\sigma_{RC,I}$	<i>N</i>	$M_K$	$\sigma_{RC,K}$
1	<0.1	all	No	3395	$(-0.206 \pm 0.011)$	$0.249 \pm 0.013$	1593	$-1.398 \pm 0.017$	$0.369 \pm 0.021$
2	<0.1	ACEFGH	No	1411	$(-0.245 \pm 0.014)$	$0.217 \pm 0.016$	436	$-1.534 \pm 0.029$	$0.277 \pm 0.036$
3	<0.1	ACEFG	No	795	$(-0.269 \pm 0.016)$	$0.205 \pm 0.018$	236	$-1.582 \pm 0.035$	$0.271 \pm 0.043$
4	<0.1, $\pi > 14.3$	ACEFG	No	182	$(-0.259 \pm 0.023)$	$0.193 \pm 0.026$	116	$(-1.624 \pm 0.025)$	$0.146 \pm 0.025$
5	<0.1, $\pi > 20.0$	ACEFG	No	86	$(-0.232 \pm 0.033)$	$0.184 \pm 0.035$	60	$(-1.628 \pm 0.033)$	$0.091 \pm 0.029$
6	<0.1	all	Yes	487	$(-0.217 \pm 0.016)$	$0.185 \pm 0.017$	245	$(-1.640 \pm 0.022)$	$0.149 \pm 0.022$
7	<0.1	ACEFGH	Yes	377	$(-0.232 \pm 0.018)$	$0.199 \pm 0.019$	210	$(-1.642 \pm 0.024)$	$0.153 \pm 0.023$
8	<0.1	ACEFG	Yes	285	$(-0.249 \pm 0.021)$	$0.206 \pm 0.023$	156	$(-1.650 \pm 0.025)$	$0.140 \pm 0.025$
9	<0.05	ACEFGH	No	716	$(-0.240 \pm 0.014)$	$0.186 \pm 0.014$	226	$(-1.651 \pm 0.024)$	$0.150 \pm 0.024$

magnitude and then fitted with the formula introduced by Paczyński & Stanek (1998):

$$N = a_1 + a_2(m - m_0) + a_3(m - m_0)^2 + \frac{a_4}{\sqrt{2\pi\sigma_{RC}^2}} \exp\left(-\frac{1}{2}\left(\frac{(m - m_0)}{\sigma_{RC}}\right)^2\right). \quad (10)$$

The results in the *K*-band are based on a subset of the selected stars in the *I*-band. In this case Eq. (10) is fitted to the stars inside the box defined by  $1.8 < (V - K) < 2.8$  and  $-3.1 < M_K < -0.1$ . The location of the boxes in a colour-magnitude diagram are illustrated in Fig. 1. An illustration of the fit of Eq. (10) to the data is shown in Fig. 2.

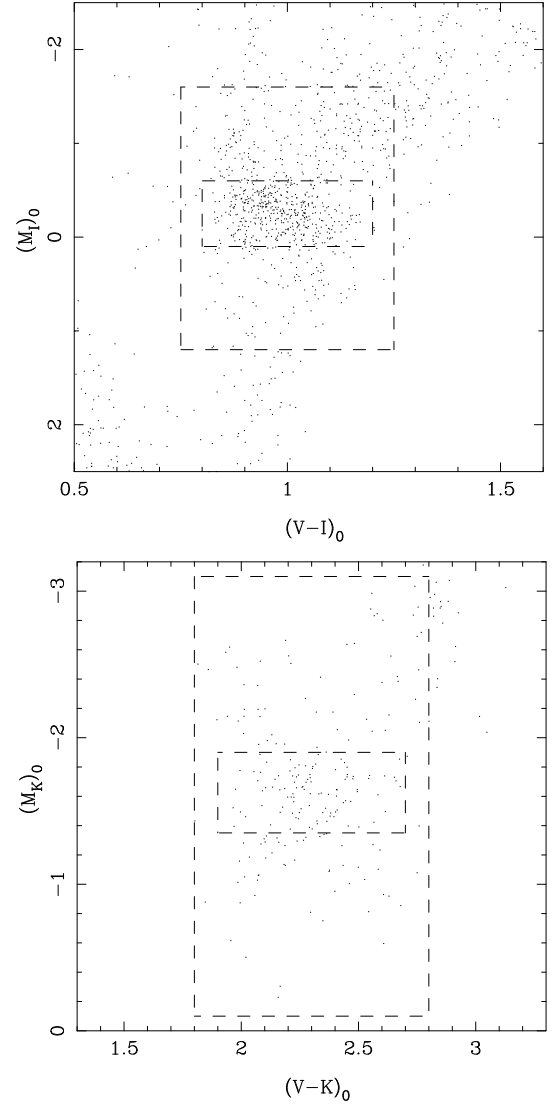
Several of the entries in Table 2 are put between parentheses, to indicate a lower quality. In the *I*-band this refers to selections that include lower-quality (*V* – *I*) data. In *K* this refers to model 5 that includes too few stars for an accurate fit of the Gaussian.

As the selection box and Eq. (10) are designed to include a “background” of stars, the fit of the absolute magnitude against colour or metallicity is made for stars that are located inside a smaller box. Based on the fit with Eq. (10) and the coefficients  $a_4, m_0, \sigma_{RC}$ , the number of red clump stars can be estimated. The location of the smaller box is chosen such that it approximately includes this number of stars. In the *I*-band this is  $0.8 < (V - I) < 1.2$  and  $-0.6 < M_I < 0.1$ . In the *K*-band this is  $1.9 < (V - K) < 2.7$  and  $-1.9 < M_K < -1.35$ .

First the dependence on colour and metallicity is investigated, fitting a linear relation. When  $M_I$  is fitted against (*V* – *I*) colour, the slope is  $0.27 \pm 0.11$ ,  $0.10 \pm 0.19$ , and  $-0.02 \pm 0.22$ , respectively, when all, “ACEFGH” and “ACEFG” Hipparcos *I*-band flags are considered. For these three selections, the slope is  $0.08 \pm 0.06$ ,  $0.06 \pm 0.07$ , and  $0.09 \pm 0.08$  when  $M_I$  is fitted against [Fe/H]. The three determinations are consistent, as one would expect since any dependence on metallicity should not depend on the origin of the *I*-band data. No significant dependence on colour is found, in accordance with Paczyński & Stanek (1998). Also the dependence on metallicity is marginal.

When  $M_K$  is fitted against (*V* – *K*) colour, the slope is  $-0.15 \pm 0.07$ ,  $-0.15 \pm 0.08$ , and  $-0.13 \pm 0.09$ , respectively, when all, “ACEFGH” and “ACEFG” Hipparcos *I*-band flags are considered. Fitted against [Fe/H], the slopes become, respectively,  $0.02 \pm 0.07$ ,  $-0.03 \pm 0.08$ , and  $-0.04 \pm 0.09$ . In *K* there is therefore no evidence of any metallicity dependence and only a marginal one on (*V* – *K*) colour.

For the selections in Table 2, the results of the simulations are listed in Table 3. As mentioned in Sect. 3.2, the input values are  $M_I = -0.27$  with  $\sigma = 0.20$ , and  $M_K = -1.60$  with  $\sigma = 0.22$ . One can observe that the bias can be up to 0.07 mag in *I* depending on the selection bias. The fifth column in Table 3 lists the “true” value, which is the observed value from Table 2, corrected by

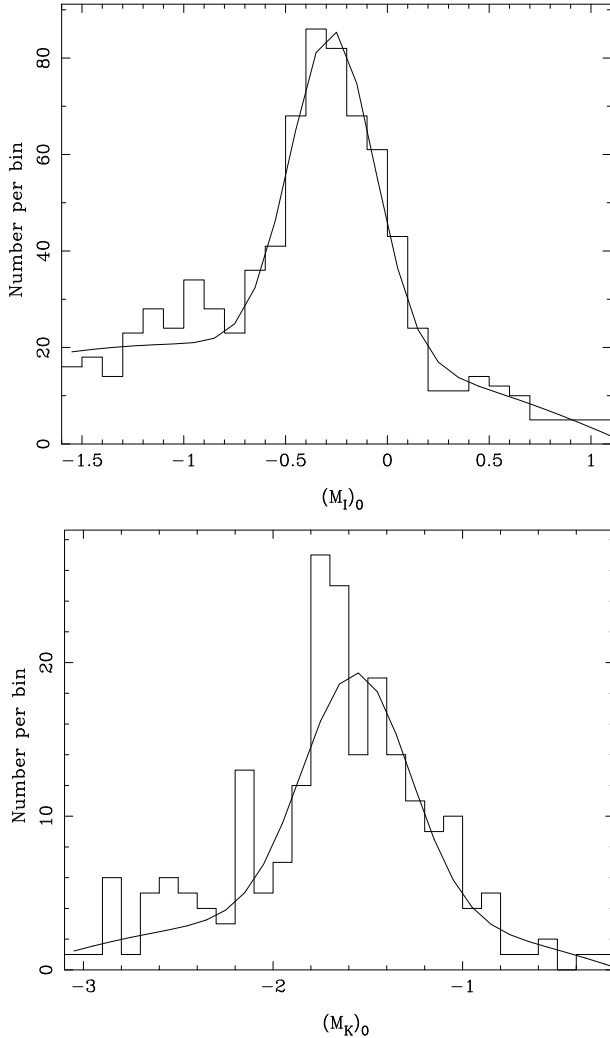


**Fig. 1.** Colour-magnitude diagrams for model 3. The outer box is used to select the data to fit Eq. (10) to. The inner box is used to fit the dependence of the absolute magnitude against colour or metallicity.

the bias, estimated from the difference between the input value and the output value from the simulation. The average of the 4 available models or the one with smallest correction (model 5) gives the identical result:  $M_I = -0.22 \pm 0.03$ . In *K* the biases are larger, up to 0.1 mag, and the average of 7 estimates is  $M_K = -1.54 \pm 0.04$ .

**Table 3.** Results of the simulations.

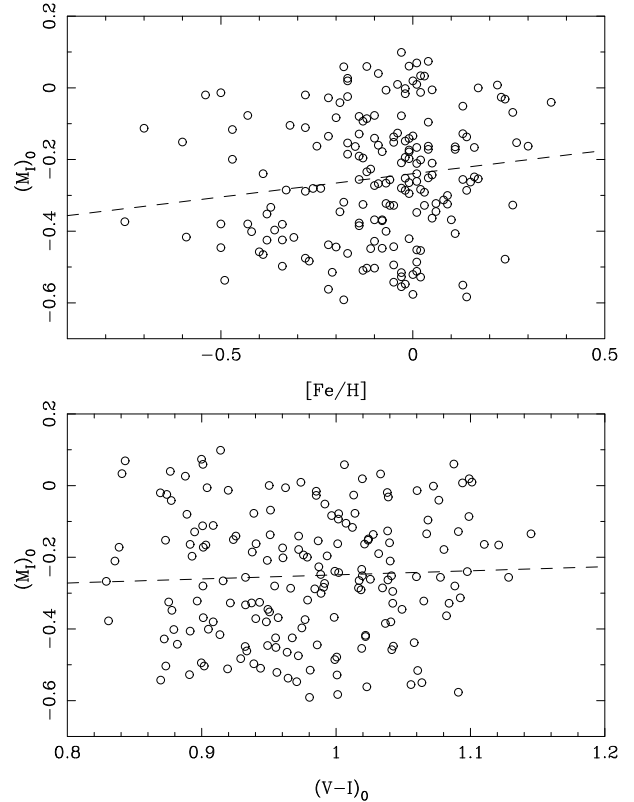
Model	$M_I$	$\sigma_{RC,I}$	$M_K$	$\sigma_{RC,K}$	$M_I$ (true)	$M_K$ (true)
2	$(-0.290 \pm 0.010)$	$0.240 \pm 0.007$	$-1.648 \pm 0.018$	$0.251 \pm 0.015$	–	$-1.486 \pm 0.034$
3	$-0.327 \pm 0.012$	$0.222 \pm 0.010$	$-1.697 \pm 0.022$	$0.238 \pm 0.021$	$-0.212 \pm 0.020$	$-1.485 \pm 0.041$
4	$-0.290 \pm 0.023$	$0.190 \pm 0.021$	$-1.625 \pm 0.035$	$0.202 \pm 0.025$	$-0.239 \pm 0.033$	$-1.599 \pm 0.043$
5	$-0.264 \pm 0.053$	$0.214 \pm 0.040$	$(-1.598 \pm 0.110)$	$0.242 \pm 0.099$	$-0.238 \pm 0.062$	–
6	$(-0.333 \pm 0.015)$	$0.218 \pm 0.011$	$-1.702 \pm 0.025$	$0.234 \pm 0.021$	–	$-1.538 \pm 0.033$
7	$(-0.337 \pm 0.018)$	$0.208 \pm 0.015$	$-1.707 \pm 0.027$	$0.233 \pm 0.029$	–	$-1.535 \pm 0.036$
8	$-0.330 \pm 0.021$	$0.217 \pm 0.018$	$-1.715 \pm 0.030$	$0.231 \pm 0.029$	$-0.189 \pm 0.034$	$-1.535 \pm 0.039$
9	$(-0.306 \pm 0.011)$	$0.210 \pm 0.009$	$-1.664 \pm 0.028$	$0.228 \pm 0.021$	–	$-1.587 \pm 0.037$

**Fig. 2.** The fit of Eq. (10) to the data in the  $I$ -band (*upper panel*), and  $K$ -band for model 3.

## 5. Summary and discussion

Using revised Hipparcos parallaxes and extensive numerical simulations that take into account the properties of the Hipparcos catalogue in terms of completeness and parallax error, and also taking into account the selection functions that are involved in selecting stars with certain properties ( $K$ -band, high-quality  $I$ -band, spectroscopic metallicities), the absolute magnitude of the red clump in  $I$  and  $K$  is investigated.

In the  $I$ -band, the value of  $M_I = -0.22 \pm 0.03$  essentially agrees with the value quoted by Stanek & Garnavich (1998). There is no dependence of  $M_I$  on  $(V - I)$  colour, and the dependence on metallicity is marginal:  $(0.08 \pm 0.07) ([Fe/H] + 0.15)$ .

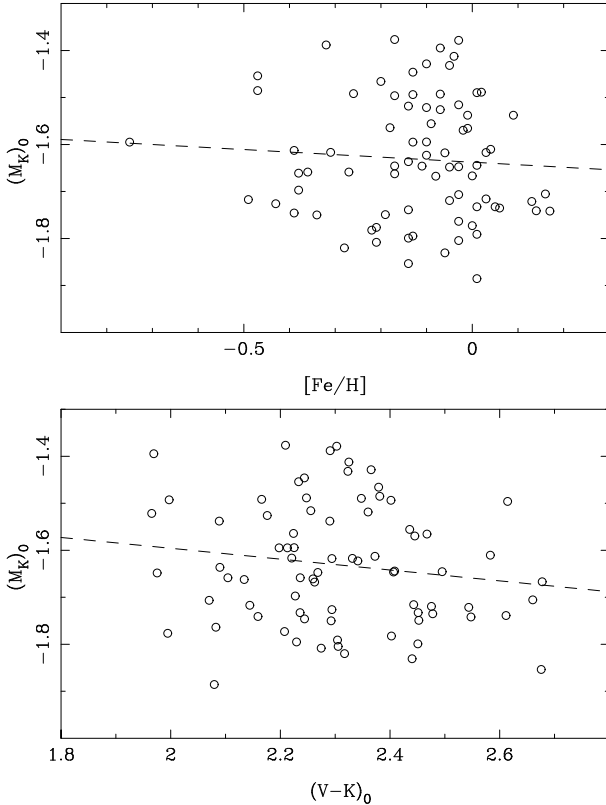
**Fig. 3.** Fit of  $M_I$  versus metallicity and  $(V - I)$  colour for model 8, with best fits indicated by the dashed line. The slope of the fit against colour is not significant.

In the  $K$ -band, the influence of selection biases appears stronger and the value derived  $M_K = -1.54 \pm 0.04$  differs significantly from the value originally derived by Alves (2000), which is almost 0.1 mag brighter, when his value of  $-1.61$  on the Bessell & Brett (1988) system is converted to the 2MASS system (Carpenter 2001). There is no dependence of  $M_K$  on metallicity, and the dependence on colour is weak:  $(-0.15 \pm 0.07) ((V - K)_0 - 2.32)$ .

The RC stars in clusters have also been used to derive  $M_K$ , originally by Grocholski & Sarajedini (2002). Absolute magnitudes are derived by combining the observed mean magnitude in a box in colour and magnitude with a reddening estimate and main-sequence fitting distances. Grocholski & Sarajedini (2002) used the second incremental data release of 2MASS and 14 clusters to find an absolute  $K$ -magnitude that is in agreement with the value in Alves (2000). Using the All-Sky data release and increasing the sample to 24 clusters, Van Helshoecht & Groenewegen (2007; hereafter vHG) find a value fainter by 0.05 mag, or  $M_K = -1.57 \pm 0.05$  on the Bessell & Brett system.

**Table 4.** The RC in old clusters.

Name	$\log t$	[Fe/H]	$M_K$	$\Delta M_K$	$M_K$ (true)
Be 39	9.90	-0.15	$-1.56 \pm 0.11$	$-0.058 \pm 0.03$	$-1.61 \pm 0.12$
NGC 188	9.63	-0.12	$-1.36 \pm 0.11$	$+0.057 \pm 0.03$	$-1.30 \pm 0.12$
NGC 6791	9.64	+0.40	$-1.39 \pm 0.11$	$+0.223 \pm 0.05$	$-1.17 \pm 0.12$
47 Tuc	10.08	-0.70	$-1.34 \pm 0.21$	$-0.360 \pm 0.11$	$-1.70 \pm 0.24$
NGC 362	10.08	-1.15	$-0.81 \pm 0.24$	$-0.680 \pm 0.11$	$-1.49 \pm 0.26$

**Fig. 4.** Fit of  $M_I$  versus metallicity and  $(V - I)$  colour for model 8, with best fits indicated by the dashed line. The slope of the fit against colour is not significant.

Both Grocholski & Sarajedini (2002) and vHG used averages over the cluster sample to arrive at the quoted means.

To compare these values to the absolute magnitude of the local Hipparcos sample, a “population correction” has to be made, to account for the difference in metallicity and age of the RC population. The calculation of this correction is outlined and tabulated in Girardi & Salaris (2001) and Salaris & Girardi (2002). In the  $K$ -band, Salaris & Girardi (2002) show that the correction is a strong function of age for ages below 3 Gyr. The top panel in their Fig. 3 shows that the correction is well behaved for ages above about 4 Gyr, and for each metallicity a linear function was fitted.

From vHG the five clusters older than 4 Gyr were taken and the population correction was determined by linear interpolation in age and [Fe/H] in the results in Salaris & Girardi. The error in  $\Delta M_K$  is based on a 1 Gyr error in age and 0.1 dex in metallicity. The results are listed in Table 4, which lists the age and metallicity (see vHG for the references for age and metallicity determination), the  $M_K$  value and its error that takes into account the error in reddening and the assumed distance to the cluster (from vHG), the population correction with error, and the corrected value. The weighted mean of the corrected  $M_K$  values

is  $-1.39 \pm 0.06$  with a dispersion of 0.2 mag. Correcting to the 2MASS system (Carpenter 2001) this becomes  $-1.43 \pm 0.06$ . Although the dispersion is large, the mean value is also fainter than the straight mean for the cluster sample and agrees within 2-sigma with the determination from the Hipparcos sample.

To settle the issue on the importance of the bias and the absolute  $K$ -magnitude of RC stars would require accurate NIR magnitudes of a 100 to a few hundred (cf. Table 2) bright ( $K \lesssim 5$ ) RC stars. Given the brightness, this represents a challenge to modern instrumentation because of saturation.

The absolute magnitudes derived here are in better agreement with theory than previously. Using a plausible star formation history for the solar neighbourhood, Salaris & Girardi (2002) derived absolute magnitudes of  $M_I = -0.17$  and  $M_K = -1.584$  (on the 2MASS system), which they compared to the Hipparcos-based results quoted in Alves et al. (2002) of  $M_I = -0.26 \pm 0.03$  and  $M_K = -1.644 \pm 0.03$  (on the 2MASS system), which indicates differences at the 2–3 sigma level. The new results of  $M_I = -0.22 \pm 0.03$  and  $M_K = -1.54 \pm 0.04$  agree with theory at the 1–2 sigma level.

Finally, some implications for existing distance determinations using the RC are discussed. The derived value of the absolute magnitude in the  $I$ -band of  $M_I = -0.22 \pm 0.03$  is not very different from previously adopted values in the literature of  $-0.23$  or  $-0.26$ , so the impact on derived distances is not so great.

The distance to the LMC quoted by Pietrzyński & Gieren (2002) of  $18.501 \pm 0.049$  (random+systematic error and assuming no population correction) based on  $JK$  observations of two fields in the bar would become  $18.35 \pm 0.05$  for an assumed population correction of  $-0.03$  (Salaris & Girardi 2002).

Babusiaux & Gilmore (2005) obtained infrared data on some fields in the direction of the Galactic bulge. Their distance scale is tied to one field for which they obtain  $M_K = -1.72$  for an assumed distance of 8 kpc. Taking  $M_K = -1.54$  would result in a distance of 7.4 kpc ( $\pm 0.2$  kpc judging from the information in their Table 2). Adding the error in  $M_K$  results in a total error of 0.3 kpc.

Using similar type of observations Nishiyama et al. (2006) obtained  $7.52 \pm 0.1$  kpc for  $M_K = -1.59 \pm 0.03$ , which translates to  $7.33 \pm 0.14$  kpc with the new DM.

This can be compared to a distance of  $7.94 \pm 0.37$  (random)  $\pm 0.26$  (systematic) kpc from Groenewegen et al. (2007) based on  $K$ -band monitoring observations of Population-II cepheids and RR Lyrae stars (distance tied to an assumed LMC distance modulus (DM) of 18.50) and the direct determination of  $7.73 \pm 0.32$  kpc based on the orbit of the star called S2 around the central black hole when post-Newtonian physics is taken into account (Eisenhauer et al. 2005; Zucker et al. 2006), although neglect of the space motion of Sgr A\* may result in systematic errors of about 0.1–0.45 kpc (Nikiforov 2008). All these independent observations are consistent and seem to indicate a DM to the GC of slightly less than 8 kpc.

*Acknowledgements.* This research has made use of the SIMBAD database, operated at CDS, Strasbourg, France.

## References

- Alves, D. 2000, *ApJ*, 539, 732  
Alves, D. R., Rejkuba, M., Minniti, D., & Cook, K. H. 2002, *ApJ*, 573, L51  
Arenou, F., Grenon, M., & Gómez, A. 1992, *A&A*, 258, 104  
Babusiaux, C., & Gilmore, G. 2005, *MNRAS*, 358, 1309  
Bessell, M., & Brett, J. M. 1988, *PASP*, 100, 1134  
Carpenter, J. M. 2001, *AJ*, 121, 2851  
Carter, B. S. 1990, *MNRAS*, 242, 1  
Dolphin, A. E., Saha, A., Skillman, E. D., et al. 2001, *ApJ*, 550, 554  
Drimmel, R., & Spergel, D. N. 2001, *ApJ*, 556, 181  
Drimmel, R., Cabrera-Lavers, A., & López-Corredoira, M. 2003, *A&A*, 409, 205  
Eisenhauer, F., Genzel, R., Alexander, T., et al. 2005, *ApJ*, 628, 246  
Epchtein, N., Deul, E., Derriere, S., et al. 1999, *A&A*, 349, 236  
ESA 1997, The Hipparcos catalogue, ESA SP-1200  
Girardi, L., & Salaris, M., 2001, *MNRAS*, 332, 109  
Girardi, L., Groenewegen, M. A. T., Hatziminaoglou, E., & da Costa L. 2005, *A&A*, 436, 895  
Grocholski, A. J., & Sarajedini A. 2002, *AJ*, 123, 1603  
Groenewegen, M. A. T., & Oudmaijer, R. D. 2000, *A&A*, 356, 849  
Groenewegen, M. A. T., Udalski A., & Bono G. 2008, *A&A*, 481, 441  
Kim, M., Kim, E., Lee, M. G., Sarajedini, A., & Geisler, D. 2002, *AJ*, 123, 244  
Koornneef, J., 1983, *A&AS* 53, 489  
Liu, Y. J., Zhao G., Shi, J. R., Pietrzyński, G., & Gieren, W. 2007, *MNRAS*, 382, 553  
Marshall, D. J., Robin, A. C., Reylé, C., Schultheis, M., & Picaud, S. 2006, *A&A*, 453, 635  
McWilliam, A. 1990, *ApJS*, 74, 1075  
Mishenina, T. V., Bienaymé, O., Gorbaneva, T. I., et al. 2006, *A&A*, 456, 1109  
Neugebauer, G., & Leighton, R. B. 1969, Two Micron Sky Survey, NASA SP-3047  
Nikiforov, I. I. 2008, [[arXiv:0803.0825](https://arxiv.org/abs/0803.0825)]  
Nishiyama, S., Nagata, T., Sato, S., et al. 2006, *ApJ*, 647, 1093  
Ochsenbein, F., Bauer, P., & Marcout, J. 2000, *A&AS*, 143, 23  
Paczynski, B., & Stanek, K. Z. 1998, *ApJ*, 494, L219  
Parenago, P. P. 1940, *Astron. Zh.*, 17, 3  
Pietrzyński, G., & Gieren, W. 2002, *AJ*, 124, 2633  
Rizzi, L., Held, E. V., Saviane, I., Tully, R. B., & Gullieuszik, M. 2007, *MNRAS*, 380, 1255  
Salaris, M., & Girardi, L. 2002, *MNRAS*, 337, 332  
Skrutskie, M. F., Cutri, R. M., Stienning, R., et al. 2006, *ApJ*, 131, 1163  
Stanek, K. Z., & Garnavich, P. M. 1998, *ApJ*, 503, L131  
Udalski, A. 2000, *ApJ*, 531, L25  
Van Helshoecht, V., & Groenewegen, M. A. T. 2007, *A&A*, 463, 559 (vHG)  
van Leeuwen, F. 2007, Hipparcos, the new reduction of the Raw Data, *ASSL* (Springer), 350  
Zhao, G., Qiu, H. M., & Mao, S. 2001, *ApJ*, 551, L85  
Zucker, S., Alexander, T., Gillessen, S., Eisenhauer, F., & Genzel, R., 2006, *ApJ*, 639, L21